A Computational Platform for Nonlinear Analysis of Prestressed Concrete Shell Structures

Kim, Tae-Hoon† Shin, Hyun Mock*

Abstract

This paper presents a formulation to include the prestressing effects in available numerical models for the nonlinear material, instantaneous and long-term analysis of prestressed concrete shell structures, based on the displacement formulation of the finite element method. A four-node flat shell element is adopted for nonlinear analysis of prestressed concrete shells. This element was incorporated into an existing general-purpose finite element analysis program. A distinctive characteristic of the element is its capability to simulate the behavior of shells subjected to a variety of types of loading and drilling rotational stiffness. Consequently, the response of prestressed concrete shell structures can be predicted accurately using the proposed nonlinear finite element procedure.

Keywords *: prestressed concrete, shell structures, nonlinear analysis, drilling rotational stiffness.*

1. Introduction

The application of the finite element method (FEM) to the analysis of concrete structures has been growing rapidly since it was first introduced by Ngo and Scordelis (1967). Because of its highly complex material behavior, the study of concrete structures by the finite element method is still under progress. Research is being carried out simultaneously both at the basic level of material characterization and for the application of the FEM for analyzing complex concrete structures (ACI, 2001; Maekawa *et al.*, 2001; Yamamoto and Vecchio, 2001; Semblat *et al.*, 2004; Smadi and Belakhdar, 2007). In this paper the application of FEM for prestressed concrete shell structures is presented.

In recent years, prestressed concrete shells have been widely applied to underground tanks, nuclear waste containers, and offshore structures. Prestressed concrete has many advantages over reinforced concrete: the behavior of the structure under service loads can be improved, cracks that might from during overloads will usually close again due to the precompression, the members can resist large shear forces, the steel has improved fatigue characteristics, and the optimum use can be made of high strength steel and concrete.

Considerable effort has been made to develop suitable finite element analysis for application to prestressed concrete shell structures (Greunen and Scordelis, 1983; Roca and Mari, 1993b; Pavic *et al.*, 2001). Much of this research has focused on developing specialized element and efficient solution algorithms, with insufficient attention to the implementation of realistic constitutive models that accurately predict the behavior of prestressed concrete shell structures.

In the present study, models were developed to address material nonlinearity by incorporating tensile, compressive and shear models for cracked concrete, in addition to including model for the reinforcing steel and tendon, which uses the smeared crack approach. The impetus in developing these models

† 책임저자, 정회원 · 삼성물산(주) 건설부문 기반기술연구소 수석연구원
Tel: 02-2145-6485 ; Fax: 02-2145-6500
E-mail: th1970.kim@samsung.com
* 종신회원 · 성균관대학교 사회환경시스템공학과 교수

• 이 논문에 대한 토론을 2011년 2월 28일까지 본 학회에 보내주시면 2011년 4월호에 그 결과를 게재하겠습니다.

was to model time dependent behavior by proper theoretical representation of the material parameters. The time dependent effects of creep, shrinkage, and relaxation of the prestressing tendon are included in the material models for the structural elements.

The primary objective of this study was to adopt a new finite element formulation for the nonlinear analysis of prestressed concrete shell structures. A formulation for the nonlinear material, instantaneous and long-term analysis of prestressed concrete shells is described, where the treatment of prestressing is achieved as a further extension of existing numerical models for reinforced concrete shells (Kim *et al.*, 2002).

In order to analyze prestressed concrete shell structures with highly nonlinear behavior, the layer method was introduced, assuming that several thin plane stress elements are layered in the direction of thickness. Thus, the developed element possesses six degrees of freedom (DOF) per node, allowing for an easy connection to other types of finite elements that have with 6-DOFs per node, a three-dimensional beam-column element, etc., and providing a much improved, more robust analysis procedure than currently exists.

The efficiency of the numerical method, and even its actual capacity to be used repeatedly for practical problems, mainly follows from the technique adopted to perform the complete geometric description. Their comparisons with available experimental or analytical results from other authors have shown both the satisfactory efficiency and reliability of the method. However, a lack of experimental studies about prestressed concrete shells has been found, meaning that experimental research is still needed regarding future verification and extension.

2. Prestressed concrete shell element

Author's previous numerical model for the nonlinear analysis of reinforced concrete shells has been adopted as a basic subtract for the later inclusion of prestressing. Its key features are briefly presented (Kim *et al.*, 2002).

The four-node isoparametric quadrilateral shell element introduced by Lanheng (1994) is chosen for the present study. The shell element is regarded as a multilayered system where each layer is assumed to be under a biaxial state of stresses. The stresses and the state of the materials vary independently at each layer to account for the mechanical changes of the materials throughout the loading process.

Presented herein is a finite element formulation for the analysis of prestressed concrete shells using a four-node quadrilateral thin flat shell finite element with 6-DOFs per node. The sixth DOF is obtained by combining a membrane element with a normal rotation, θ_z, the so-called drilling degree of freedom, and a discrete Kirchhoff plate element. These modeling assumptions are shown in Fig. 1

In order to analyze prestressed concrete shells with nonlinear behavior, the layer method was used, assuming that several thin plane stress elements are layered in the direction of thickness. In the layered element formulation, the shell is divided into several paneled layers and two-dimensional constitutive models were applied to take into account material nonlinearities. This technique allows for the addition of any number of additional layers of steel with

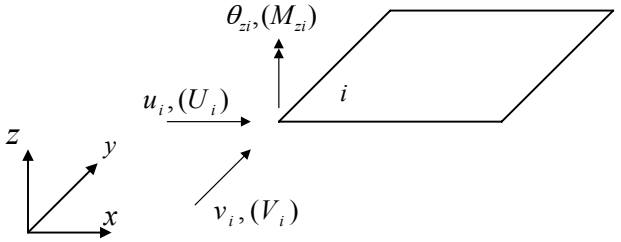

(a) Plane membrane actions and deformations

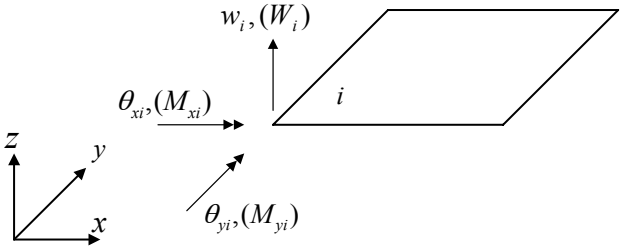

(b) Bending actions and deformations

Fig. 1 A flat shell element subjected to plane membrane and bending action

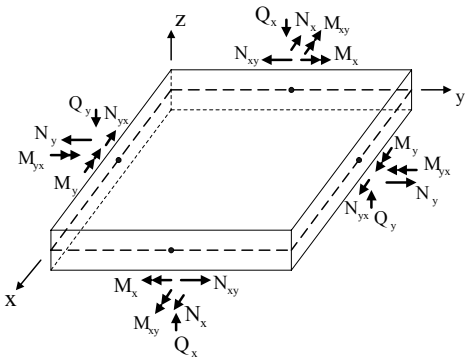

(a) Forces acting on PSC shells

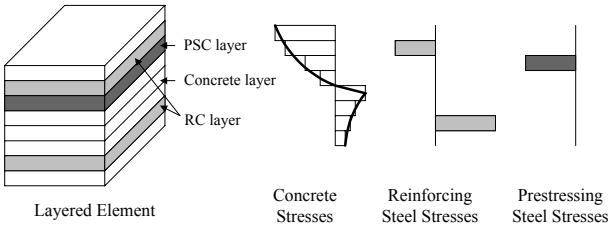

(b) Layered element

Fig. 2 Shell element

different orientations to be added to finite element model. Fig. 2 illustrates the layered element and forces acting on the shells.

The prestressing technique has been more and more employed in concrete constructions demanding an efficient modeling of the contribution of prestressing tendon to the structural equilibrium equations. The conventional way of treating steel bars in prestressed concrete shells is as an equivalent layer smeared over the entire area of the shells.

Most of the formulations presented up to now which include prestressing have been developed as an extension of existing models for the analysis of reinforced concrete structures, and agree in their main features (Wu *et al.*, 2001). However, so far this application has found a practical limitation in the lack of available experimental results to be used for the verification (Roca and Mari, 1993a).

In this study, prestressing is considered as an initial unbalanced stress and an equivalent load system is evolved and applied in the opposite direction to find the deformations and stresses in the structure due to prestressing.

An automatic procedure has been also developed

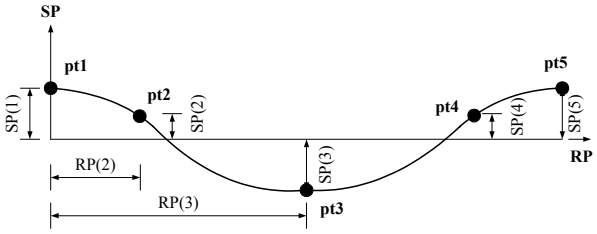

Fig. 3 Basic span for tendon geometry generation

that, using a set of analytical expressions as primordial data to describe the shell and the courses of the tendons, later generates a global geometric interpolation. The interpolation of the tendon courses is dependent to the isoparametric interpolation of a shell element. This application to concrete shell structures has one of its more important aspects in the need to minimize the input data preparation for the complete definition of the geometry of the problem, including the shell middle surface and the space curves that refer the axis of prestressing tendons.

Prestressing tendons with arbitrary tendon profiles are modeled with a number of piecewise linear tendon segments defined by tendon points (see Fig. 3). Each tendon point is associated with a node, to which its displacements are rigidly constrained. The global coordinates of the tendon points may be input directly or may be generated automatically using a parametric generation scheme. The prestressing tendons may be stressed, restressed or removed at any stage of the solution.

3. Nonlinear material model for prestressed concrete

The nonlinear material model for the prestressed concrete is composed of models to characterize the behavior of the concrete, in addition to models for characterizing the reinforcing bars and tendons (see Fig. 4). Models for concrete may be divided into models for uncracked concrete and cracked concrete. The basic model adopted for crack representation is a non-orthogonal fixed-crack method of the smeared crack concept, which is widely known to be a model

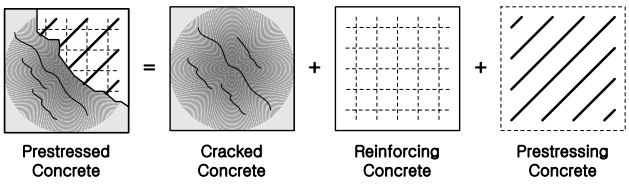

Fig. 4 Prestressed concrete shell element model

for crack representation.

This section includes summary of the material models used in the analysis. A full description of the nonlinear material model for reinforced concrete is given by authors (Kim *et al.*, 2002; 2003).

3.1 Model for uncracked and cracked concrete

The elasto-plastic and fracture model for the biaxial state of stress proposed by Maekawa and Okamura (1983) is used as the constitutive equation for uncracked concrete.

After concrete cracks, the behavior becomes anisotropic in the crack direction. The stress-strain relations are modeled by being decomposed in directions parallel to, along and normal to cracks, respectively. Thus, the constitutive law adopted for the cracked concrete consists of tension stiffness, compression and shear transfer models. To obtain a more accurate tension stiffness model, the tensile stresses of concrete are transformed into the components in the direction normal to the crack; this is especially true when the reinforcing ratios in orthogonal directions are significantly different and when the reinforcing bars are distributed only in one direction. A modified elasto-plastic fracture model is used to describe the behavior of concrete in the direction of the crack plane. The model describes the degradation in compressive stiffness by modifying the fracture parameter in terms of the strain perpendicular to the crack plane. The shear transfer model based on the contact surface density function (Li and Maekawa, 1988) is used to consider the effect of shear stress transfer due to the aggregate interlock at the crack surface. The contact surface is assumed to respond elasto-plastically, and the model is applicable to any arbitrary loading history.

3.2 Model for the reinforcing bars in concrete

The stress acting on the reinforcing bar embedded in concrete is not uniform and the value is at maximum at locations where the bar is exposed to a crack plane. The constitutive equations for the bare bar may be used if the stress-strain relation remains in the elastic range. The post-yield constitutive law for the reinforcing bar in concrete considers the bond characteristics and the model is a bilinear model.

Kato's model (1979) for the bare bar under the reversed cyclic loading and the assumption of stress distribution denoted by a cosine curve were used to derive the mechanical behavior of reinforcing bars in concrete under the reversed cyclic loading.

3.3 Model for the prestressing tedons in concrete

Bilinear diagrams used to characterize the mild steel behavior, showing a brusque yielding, are not immediately extrapolable to prestressing tendons. For prestressing tendons, which does not have a definite yield point a multilinear approximation may be required. High strength steel used for prestressing shows a rather large proportional behavior followed by a progressive yielding. To simulate such a behavior, Kang (1977) and Mari (1984) used a multilinear diagram of five branches. In this study, the modified

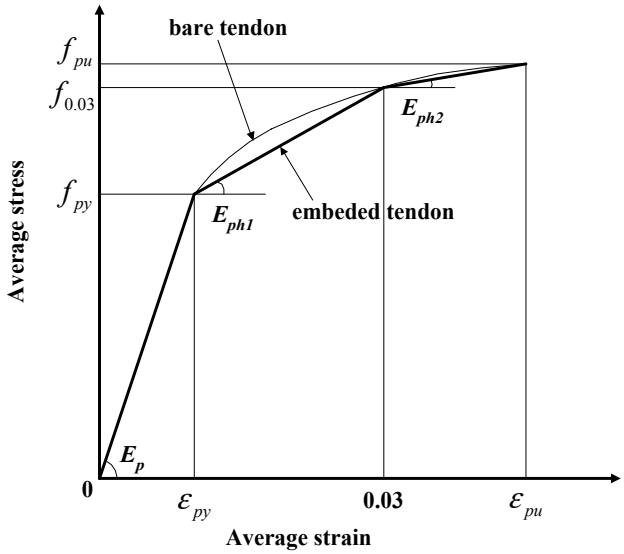

Fig. 5 Model for tendons

modeling is adopted for the present formulation as follows (see Fig. 5). A trilinear model for the stress-strain relationship of prestressing tendon considering the bond effect has been used. Unloading and reloading processes are accounted for through straight branches with the initial modulus.

$$\sigma_{pt} = f_{py} + E_{ph1}(0.03 - \varepsilon_{py}) + E_{ph2}(\varepsilon_{pu} - 0.03) \quad (1)$$

$$E_{ph1} = \frac{f_{0.03} - f_{py}}{0.03 - \varepsilon_{py}} \quad (2)$$

$$E_{ph2} = \frac{f_{pu} - f_{0.03}}{\varepsilon_{pu} - 0.03} \quad (3)$$

where σ_{pt} =stress of tendon; f_{py} =yielding strength of tendon; f_{pu} =ultimate strength of tendon; ε_{py} =yielding strain of tendon; ε_{pu} =ultimate strain of tendon; and E_{ph1}, E_{ph2} =strain hardening rates of the tendon embedded in concrete.

4. Modeling for the time dependent behavior of prestressed concrete structures

Concrete is unique among structural materials in that it undergoes complex physical and chemical changes over time, resulting in deformations and constitutive properties which are time dependent under practical service condition. Accurate consideration of time dependent concrete behavior is necessary for the accurate prediction of stresses and deflections in the structure at all load levels.

Creep, relaxation and shrinkage are time-related phenomena that may affect the mechanical behavior of normal materials under service load conditions: creep is a progressive increase in strain under sustained loading, relaxation is the dual phenomenon; it corresponds to a stress decrease under constant strain conditions, and shrinkage is volumetric self-contraction of the unconstrained material.

For the quasi-static time-dependent analysis, the time domain is divided into a discrete number of intervals, and a step-forward integration is performed in which increments of displacements, strains and stressed are successively added to the previous totals as the solution progresses in the time domain. At each time step, a direct stiffness analysis based on the displacement method is performed in the space domain in which the equilibrium equations to be solved are necessarily nonlinear due to various material nonlinearities considered.

4.1 Time dependent effect

An important assumption in studying and predicting the time dependent behavior of prestressed concrete structures is that the total strain in the concrete may be considered as a superposition of several independent components caused by different phenomena.

The nonmechanical strains (ε^{nm}) are introduced and defined as the part of the total strains (ε), which are obtained in addition to that which would have obtained in an instantaneous analysis (ε^{m})

$$\varepsilon = \varepsilon^{m} + \varepsilon^{nm} \quad (4)$$

Formally, the nonmechanical strains (ε^{nm}) can be treated as the initial strains so that the equilibrium condition, as introduced by the virtual work equation.

The following individual contributions are considered as part of the nonmechanical strains: concrete creep (ε^{c}), concrete shrinkage (ε^{s}), concrete ageing (ε^{a}), and possible strains due to thermal effects (ε^{t}). Just as an approach, superposition is assumed thus neglecting their actual coupling

$$\varepsilon^{nm} = \varepsilon^{c} + \varepsilon^{s} + \varepsilon^{a} + \varepsilon^{t} \quad (5)$$

Creep and shrinkage strains (ε^{c} and ε^{s}) in concrete are influenced by a number of factors depending on the mix design, the loading history, and the environment. Ageing strain (ε^{a}) is a fictitious stress originated strain which can be defined as the decrease in mechanical strain over time due to the increase in elastic modulus of the concrete. Temperature strain

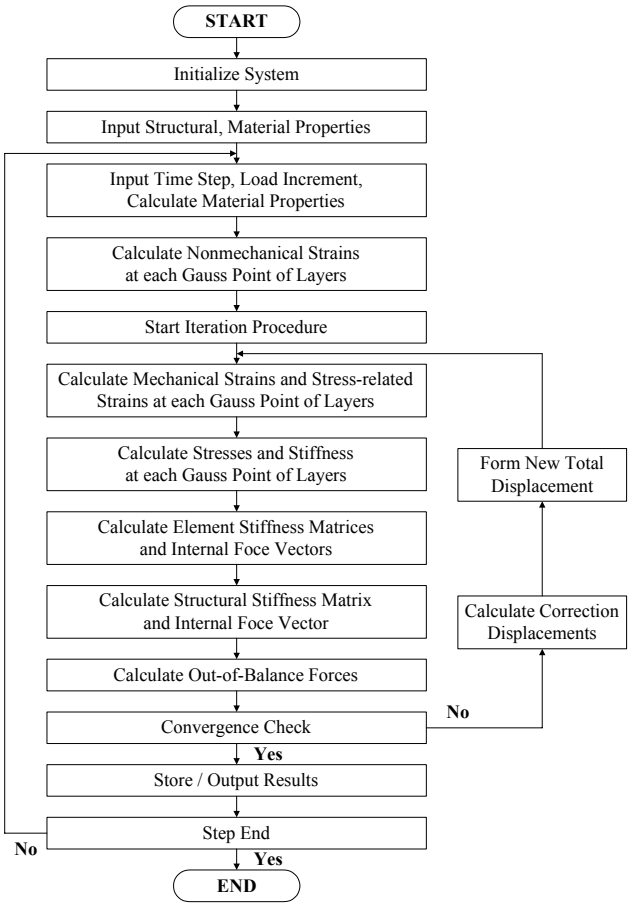

Fig. 6 Flowchart for creep and shrinkage

(ε^t) is a non-stress originated strain defined as the deformation under temperature change. The overall algorithm of the complete procedure is briefly described in Fig. 6.

4.2 Model for the creep of concrete

Creep of concrete presents one of the most complex numerical problems in the time dependent analysis of prestressed concrete structures. The main factors influencing the creep of concrete are compressive strength, age at loading, aggregate type, ambient relative humidity and temperature, the specimen size, and the stress history.

Improved creep analysis model developed by Kang (1989) is incorporated. The creep data can be generated automatically by the program utilizing ACI (1992) recommendations. The ACI recommendations are provided in the equation from required for computer analysis.

Creep strain at any time under constant stress is computed using the following expression.

$$C(t) = K_S K_H K_h K_t \frac{(t-\tau)^{0.60}}{10+(t-\tau)^{0.60}} C_u \tag{6}$$

where $C(t)$ =creep coefficient=(creep strain at any time t/initial instantaneous strain); C_u =ultimate creep coefficient determined from experiments; K_S =slump correction factor(=$0.81+0.07s$); K_H =humidity correction factor(=$1.27-0.0067H$, $H>40\%$); H =relative humidity; K_h =minimum thickness correction factor (=$1.0-0.0167(th-6.0)$, $th>6$ inches); K_t =age at loading correction factor(=$1.25\tau^{-0.118}$ for 7 days moist cured concrete); s =slump in concrete; th =minimum size of member in inches; t =observation time in days; and τ =age at loading in days.

4.3 Model for the shrinkage of concrete

Shrinkage of concrete is due primarily to loss of water upon drying (drying shrinkage) and volume change due to carbonation (carbonation shrinkage). The main factors influencing the shrinkage of concrete are aggregate type, water-cement ratio, specimen size, and ambient relative humidity.

Shrinkage strain is computed using the following relationship.

$$\varepsilon^s(t) = \varepsilon^s{}_u K_S K_h K_H \frac{(t-t_0)^e}{f+(t-t_0)^e} \tag{7}$$

where $\varepsilon^s(t)$ =shrinkage strain at observation time, t; $\varepsilon^s{}_u$ =ultimate shrinkage strain determined from experiments; t =time at observation; t_0 =age of curing; f, e =constants determined from experiments; K_S =slump correction factor; K_h =member size correction factor; and K_H =relative humidity correction factor.

4.4 Model for the relaxation of prestressing tendon

As experimentally stated, tensioned steel shows a delayed decrease of force when the length of the tendon is kept constant. The magnitude of the force loss depends mainly on the initial stress level in the tendon and on the service temperature.

A direct mathematic formulation developed by Magura *et al.* (1964) and previously utilized by Kang (1977) is adopted for the present work as well. The model uses the following experimental formula

$$\frac{\sigma_p}{\sigma_{pi}} = 1 - \frac{\log_{10} t}{c}\left[\frac{\sigma_{pi}}{\sigma_{py}} - 0.55\right], \quad \text{for} \frac{\sigma_{pi}}{\sigma_{py}} \geq 0.55 \tag{8}$$

where σ_p =predicted final stress for an initial stress σ_{pi} and after t days; σ_{py} =steel yielding stress; and c=constant(10 for stress-relieved tendon, 45 for low-relaxation tendon).

5. Numerical examples

The presented formulation has been implemented into computer as an extension of the existing program RCAHEST (Reinforced Concrete Analysis in Higher Evaluation System Technology), previously developed for the nonlinear analysis of reinforced concrete structures (Kim and Shin, 2001). The program is built around the finite element analysis program shell named FEAP, developed by Taylor (2000). Three numerical examples are presented through which, by comparison with existing experimental results, the efficiency and the reliability of the method are shown.

5.1 Elements subjected to in-plane shear force

Marti and Meyboom (1992) conducted an experimental work in which panel specimens with partial prestressing were tested, as shown in Fig. 7. The three specimens were identical except for the reinforcement in one direction. In this direction, one specimen was nonprestressed while its two companion specimens were partially prestressed to various degrees.

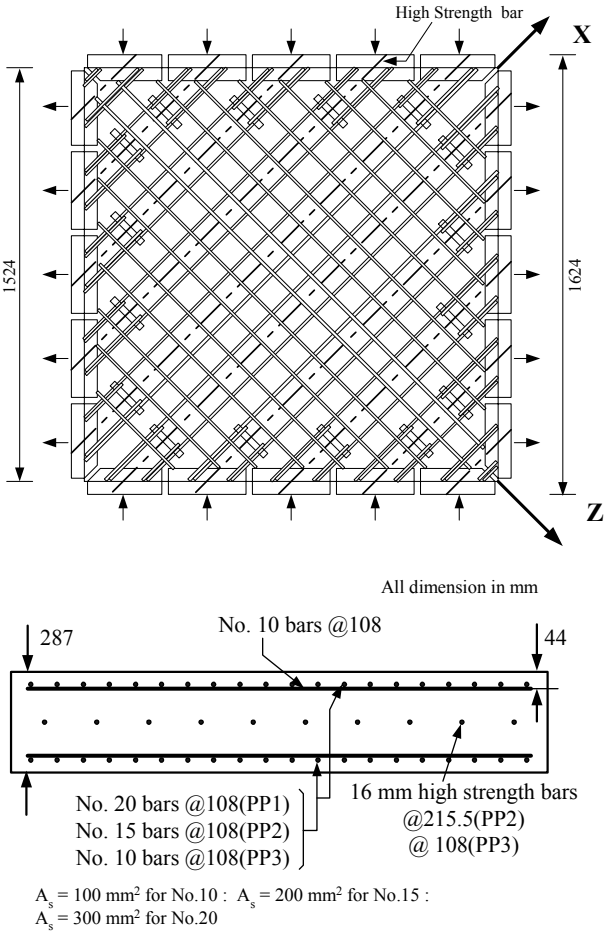

Fig. 7 Application of stresses of specimens and reinforcement layout

Table 1 Main specimen properties (Marti and Meyboom, 1992)

Specimen		PP1	PP2	PP3
Prestress in x-direction (MPa)		0	2.07	4.40
Concrete	$f_c^{'}$ (MPa)	27.0	28.1	27.7
Reinforcement	ρ_{px} (%)	-	0.293	0.586
	f_{yp} (MPa)	-	910	910
	ρ_x (%)	1.942	1.295	0.647
	f_{yx} (MPa)	479	486	480
	ρ_z (%)	0.647	0.647	0.647
	f_{yz} (MPa)	480	480	480

The main specimen properties are summarized in Table 1.

Because the force distribution is uniform across the element, only one finite element was used to predict the response of the specimen, and the number of layers used for per element was three. The resulting

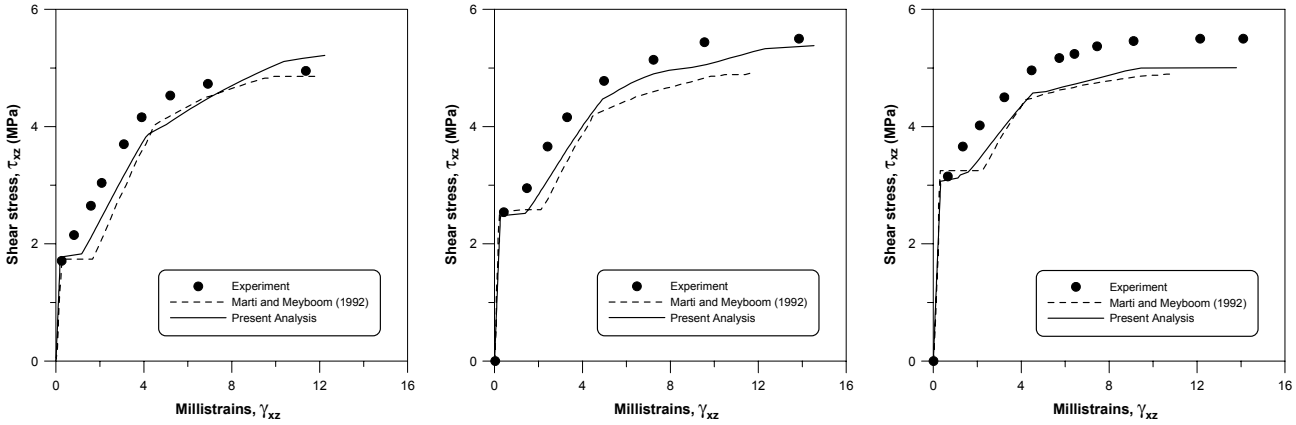

(a) PP1 (b) PP2 (c) PP3

Fig. 8 Predicted and measured load-deformation response for specimens

Table 2 Comparison of experimental and analytical results (unit:MPa)

Specimen		PP1			PP2			PP3		
		Exp. (1)	Ana. (2)	(1)/(2)	Exp. (1)	Ana. (2)	(1)/(2)	Exp. (1)	Ana. (2)	(1)/(2)
Cracking		1.71	1.67	1.02	2.54	2.48	1.02	3.15	3.07	1.03
Yielding	ρ_x	-	-	-	5.47	5.33	1.03	5.43	5.00	1.09
	ρ_z	4.24	4.41	0.96	4.41	4.84	0.91	4.92	4.78	1.03
Ultimate		4.95	5.32	0.93	5.50	5.49	1.00	5.50	5.04	1.09

load-deformation response for specimens is presented in Fig. 8 and Table 2, together with test results and analytical results. It can be seen that the generation of cracks, yielding of steels, and ultimate strength were predicted with good agreements. An exception was in the case of specimen PP3, where the prediction of ultimate strength was lower than the experimental result. The satisfactory results of previous analysis by Marti and Meyboom (1992) have been improved.

Compared to nonprestressed elements, prestressing results in higher cracking loads, reduced crack reorientation of the internal forces after cracking, delayed degradation of the concrete strength, lager strains in the reinforcement at ultimate, and higher ultimate loads.

5.2 Prestressed concrete containment structure

To verify the present analysis in a complete system made up of shell elements, the containment structure tested by Rizakalla *et al.* (1984) were used as the basis for comparison. The test structure consisted of

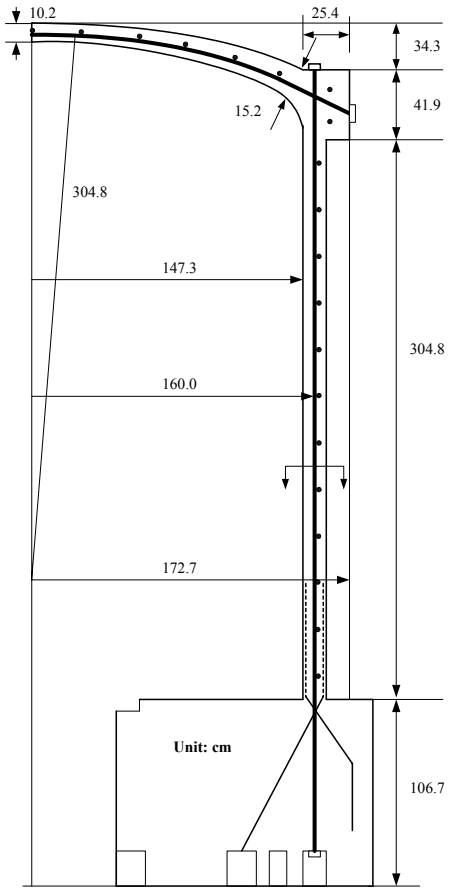

Fig. 9 Vertical section through test structure (Rizakalla *et al.*, 1984)

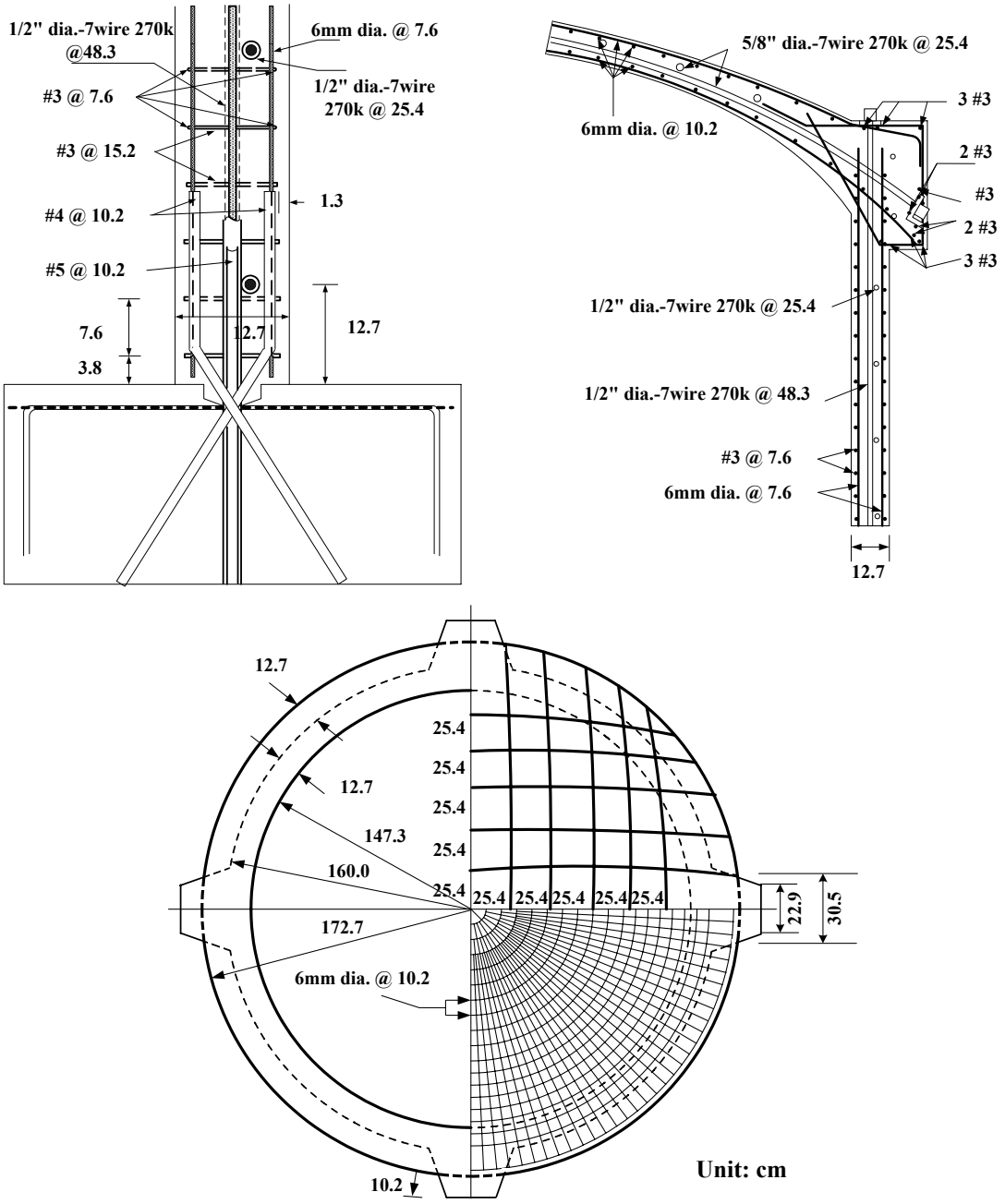

Fig. 10 Reinforcement details(Rizakalla *et al.*, 1984)

a reinforced concrete base, cylindrical wall, ring beam and dome built of prestressed concrete with construction details patterned after the Canadian CANDU reactor containment (see Fig. 9 and Fig. 10). An overall scale of 1:14 was selected as a convenient size to be tested in the laboratory. In this test, internal pressure was obtained using water and was proportionally increased until failure occurred. The material properties of specimen are given in Table 3.

Fig. 11 shows the finite element discretization and the boundary conditions for nonlinear analysis of the prestressed concrete containment structure. The structure is divided into 170 elements. The Fig. 12 shows a comparison between the experimental and analytical behavior for this test. The analysis predicted well the envelope curve of load-deflection for both the wall and dome.

A comparison of measured and predicted strains

Table 3 Material properties

Item			Specimen
Concrete	$f_c^{'}$ (MPa)		30.0
	ν		0.15
Reinforcement	6mm bar	f_y (MPa)	482 (Meridional)
	#3 bar	f_y (MPa)	345 (Circumferential)
Tendon	f_{pu} (MPa)		1,864
	f_{py} (MPa)		1,586
	ε_{pe}		0.00316
	E_s (Gpa)		200

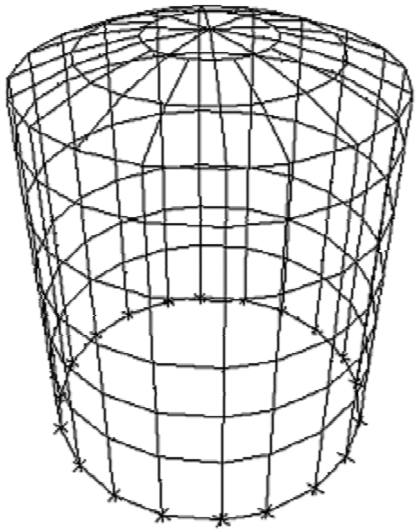

Fig. 11 Finite element mesh for analysis.

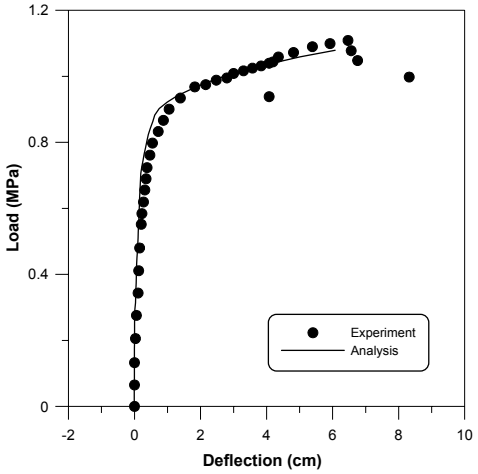

(a) Wall

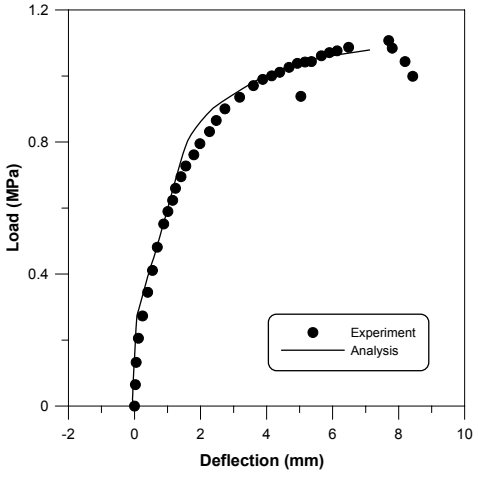

(b) Dome

Fig. 12 Pressure versus deflection

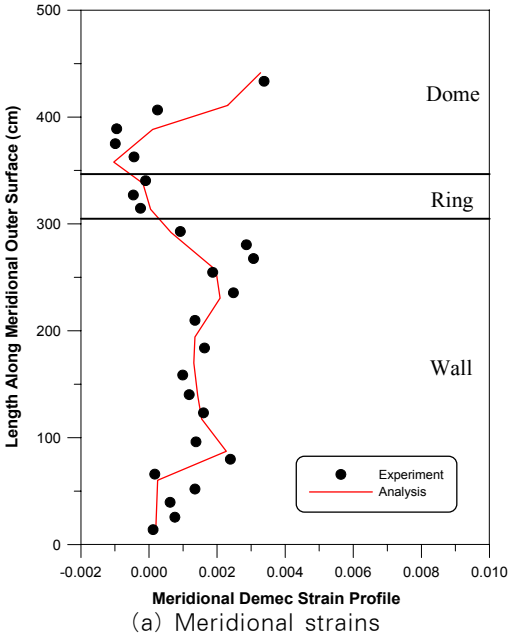

(a) Meridional strains

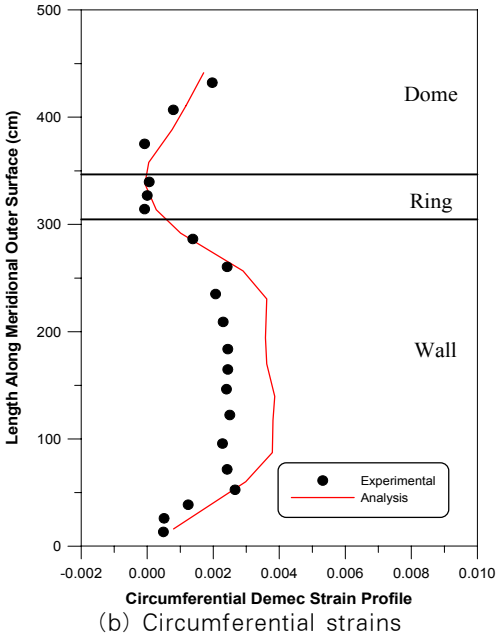

(b) Circumferential strains

Fig. 13 Measured and computed strains at 0.83MPa

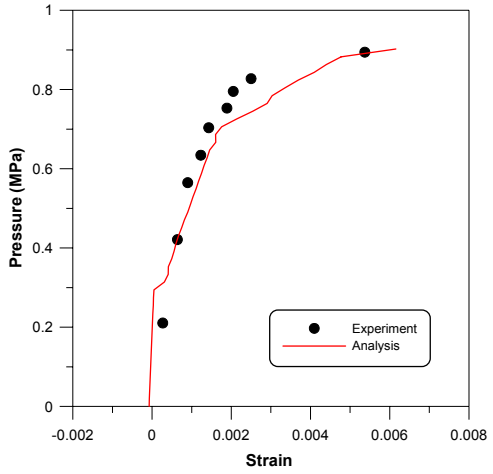

Fig. 14 Measured and computed circumferential strains in wall at 165cm above base

along the meridian and the circumferential strains across this meridian are given in Fig. 13(a) and (b), respectively, for an internal pressure of 0.83MPa. In general, the agreement is very close. The apparent large differences in circumferential strains at midheight of the wall can be better interpreted by examining the load-strain curve for the gage at midheight given in Fig. 14. The horizontal difference in Fig. 13(b) is the same distance between measured and computed values in Fig. 14 for a pressure of 0.83MPa. Note that it is suggested that future work will require further experimental and theoretical research.

The test structure has verified the ductile behavior expected in such a structure and has verified the predictive capability of the analyses developed in this study. These, in turn, have been used to predict ultimate capacity and leakage of the prototype at various stages in its loading history.

5.3 Long-term behavior of the prestressed members

The objectives of the selected experimental program (Chiu *et al.*, 1996) are to check the accuracy of the constitutive modeling for time-dependent analysis of prestressed concrete shell structures in this study. Prestressed concrete beams were cast to investigate the long-term behavior of the prestressed members under effects of creep and shrinkage. These specimens, with dimensions of 150mm×200mm×4000mm, were cast in the laboratory as shown in Fig. 15. The prestressing tendons were straight and located 11cm from the top face of the beam. The material properties of the specimens are listed in Table 4 and Table 5.

This experiment consisted of four specimens. The first one was the control specimen which was not subjected to any loading and prestress (SB03B). The second and the third ones were subjected to the prescribed loading and prestress (SB13B, SB13C). The last specimen was the same as SB13B except for the loading age of 7 day (SB17B). Additionally, in order to understand the behavior of unloading and recovery, specimen SB17B was unloaded after 117 day. The parameters for each specimen were summarized in Table 6.

Table 4 Modulus of elasticity and compressive strength (Chiu *et al.*, 1996)

Age of test (day)	Cylinder strength $f_c^{'}$ (MPa)	Modulus of elasticity E_c (MPa)
3	27.4	19123
7	33.7	21967
28	45.7	23536

Table 5 Material property of prestressing tendon (Chiu *et al.*, 1996)

Diameter (mm)	Area of cross section (mm^2)	Yield loading (kN)	Failure stress (MPa)	Rate loose (%)
12.83	100.27	173.5	1931.8	0.54

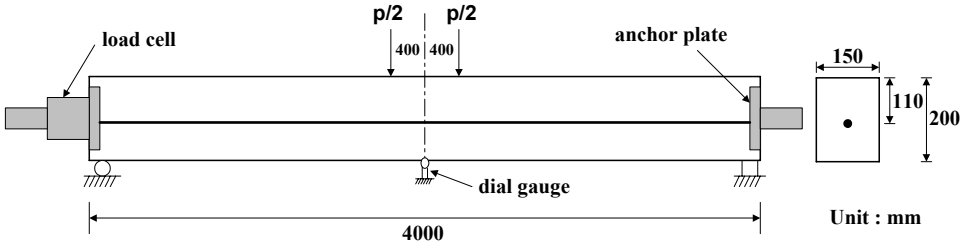

Fig. 15 Flexural test setup (Chiu *et al.*, 1996)

Table 6 Parameters of flexure experiment (Chiu *et al.*, 1996)

Specimen	Initial prestress (kN)	Age (day)	Loading (kN)	Factors	
				Creep	Shrinkage
SB03B	-	3	-	Yes	Yes
SB13B	97.3	3	2.87	Yes	Yes
SB13C	100.7	3	2.86	Yes	No
SB17B	107.9	7	2.86	Yes	Yes

This analysis modeled the specimens using mesh of 10 elements. The shell element was divided into 10 layers through the thickness. The comparison between analytical and experimental results is shown in Fig. 16(a) to (d). The analytical results show a good agreement with the experimental results, not only in regards to loading, but also in unloading.

6. Conclusions

A formulation has been presented for the nonlinear material, instantaneous and long-term analysis of prestressed concrete shell structures. Such a formulation is based on the four-node quadrilateral flat shell element with drilling rotational stiffness. In order to analyze prestressed concrete shells with nonlinear behavior, this study introduces the layer method, which assumes that several thin plane stress elements are layered in the direction of thickness. Prestressing is considered as an internal force on the element. This consistency, together with some practical implementation considerations, makes it possible to use the proposed formulation to include the numerical

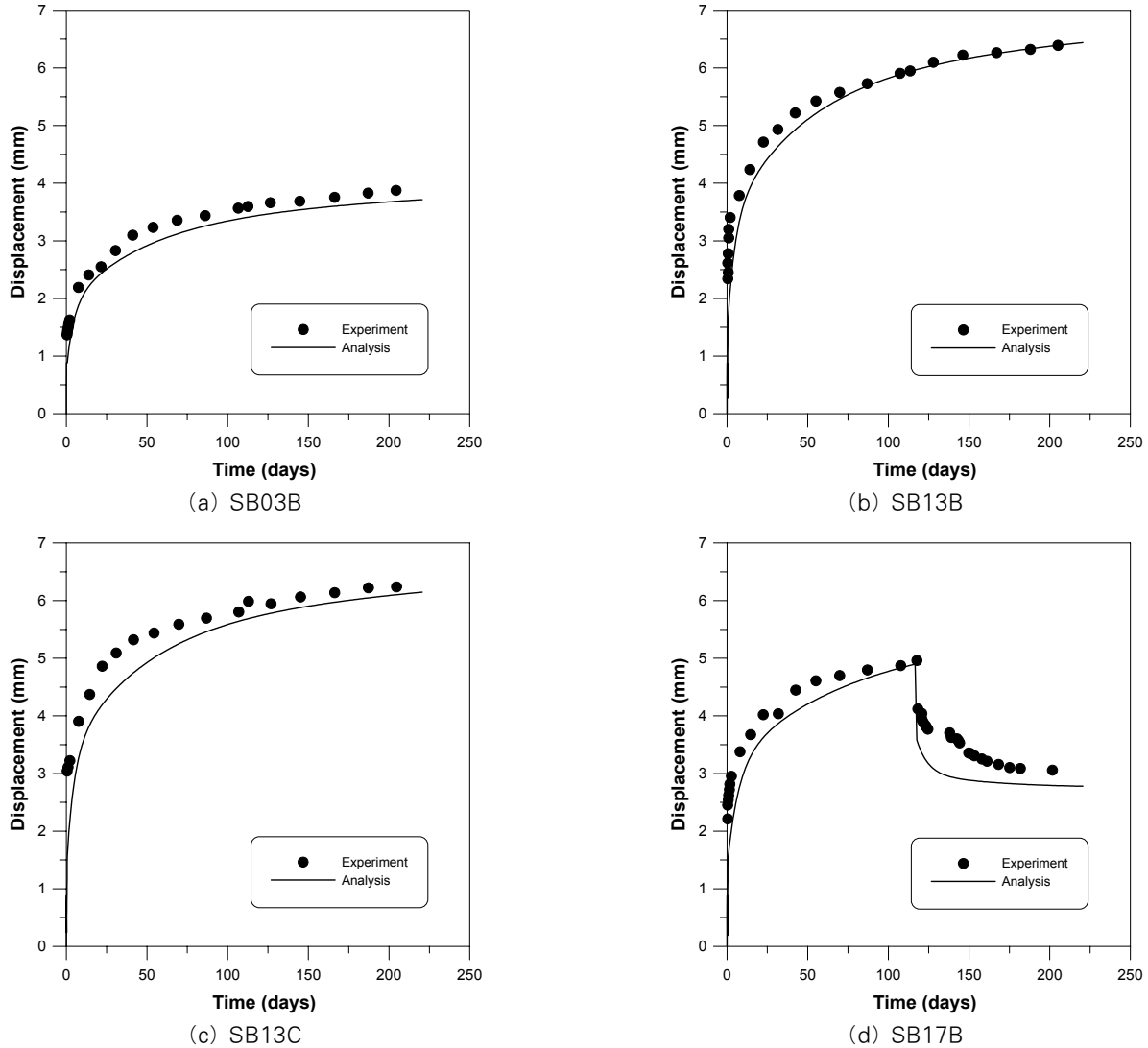

(a) SB03B (b) SB13B

(c) SB13C (d) SB17B

Fig. 16 Displacement at the middle of beam versus time

treatment of prestressing in many existing numerical models previously developed for reinforced concrete shells. Thus, the adopted element predicts with reasonable accuracy the behavior of prestressed concrete shells subjected to a variety of types of loading.

The results obtained with the numerical model in the case of three examples of application are presented and compared with experimental and analytical results from other authors. Through those examples, the capability of the numerical model to realistically represent the nonlinear behavior of prestressed concrete shell structures throughout their initial, cracked and ultimate ranges is shown. However, some are detected that require further experimental and theoretical research.

The resulting presented program has proved to be very effective in clarifying the structural behavior under increased and sustained loads. It can be used in structural analysis or as a powerful research tool, complementing experimental investigations, for defining more precise practical rules to be adopted in the design of prestressed concrete shell structures.

References

ACI (2001) *Finite Element Analysis of Reinforced Concrete Structures*.

ACI Committee 209 (1992) Prediction of Creep, Shrinkage and Temperature Effects in Concrete Structures, ACI 209R-92.

Chiu, H.S., Chern, J.C., Chang, K.C. (1996) Long-term Deflection Control in Cantilever Prestressed Concrete Bridges. Ⅱ: experimental verification, *Journal of Engineering Mechanics*, ASCE, 122(6), pp.495~501.

Greunen, J.V., Scordelis, A.C. (1983) Nonlinear Analysis of Prestressed Concrete Slabs, *Journal of Structural Engineering*, ASCE, 109(7), pp.1742~1760.

Kang, Y.J. (1977) Nonlinear Geometric, Material and Time Dependent Analysis of Reinforced and Prestressed Concrete Frames, *UC-SESM Report No. 77-1*, University of California, Berkeley.

Kang, Y.J. (1989) SPCFRAME-Computer Program for Nonlinear Segmental Analysis of Planar Prestressed Concrete, *UC-SESM Report No. 89-07*, University of California, Berkeley.

Kato, B. (1979) Mechanical Properties of Steel Under Load Cycles Idealizing Seismic Action, *CEB Bulletin D'Information*, 131, pp.7~27.

Kim, T.H., Lee, K.M., Shin, H.M. (2002) Nonlinear Analysis of Reinforced Concrete Shells Using Layered Elements with Drilling Degree of Freedom, *ACI Structural Journal*, 99(4), pp.418~426.

Kim, T.H., Lee, K.M., Yoon, C.Y., Shin, H.M. (2003) Inelastic Behavior and Ductility Capacity of Reinforced Concrete Bridge Piers Under Earthquake. Ⅰ: theory and formulation, *Journal of Structural Engineering*, ASCE, 129(9), pp.1199~1207.

Kim, T.H., Shin, H.M. (2001) Analytical Approach to Evaluate the Inelastic Behaviors of Reinforced Concrete Structures Under Seismic Loads, *Journal of the Earthquake Engineering Society of Korea*, EESK, 5(2), pp.113~124.

Lanheng, J. (1994) Analysis and Evaluation of a Shell Finite Element with Drilling Degree of Freedom, *Masters Thesis*, University of Maryland, College Park, Md.

Li, B., Maekawa, K. (1988) Contact Density Model for Stress Transfer Across Cracks in Concrete, *Concrete Engineering*, JCI, 26(1), pp.123~137.

Maekawa, K., Okamura, H. (1983) The Deformational Behavior and Constitutive Equation of Concrete Using Elasto-Plastic and Fracture Model, *Journal of the Faculty of Engineering*, University of Tokyo, 37(2), pp.253~328.

Maekawa, K., Pimanmas, A., Okamura, H. (2001) *Nonlinear Mechanics of Reinforced Concrete*, SPON Press.

Magura, D.D., Sozen, M.A., Siess, C.P. (1964) A Study of Stress Relaxation in Prestressing Reinforcement, *PCI Journal*, 9(2), pp.13~57.

Mari, A.R. (1984) Nonlinear Geometric, Material and Time Dependent Analysis of Three Dimensional Reinforced and Prestressed Concrete Frames, *UC-SESM Report No. 84-12*, University of California, Berkeley.

Marti, P., Meyboom, J. (1992) Response of Prestressed Concrete Elements to In-Plane Shear Forces, *ACI Structural Journal*, 89(5), pp.503~514.

Ngo, D., Scordelis, A.C. (1967) Finite Element Analysis of Reinforced Concrete Beams, *Proceedings*,

ACI, 64(3), pp.152~163.

Pavic, A., Reynolds, P., Waldron, P., Bennett, K. (2001) Dynamic Modelling of Post-Tensioned Concrete Floors using Finite Element Analysis, *Finite Element in Analysis and Design*, 37(4), pp.305~323.

Rizakalla, S.H., Simmonds, S.H., MacGregor, J.G. (1984), Prestressed Concrete Containment Model, *Journal of Structural Engineering*, ASCE, 110(4), pp.730~743.

Roca, P., Mari, A.R. (1993a) Numerical Treatment of Prestressing Tendons in the Nonlinear Analysis of Prestressed Concrete Structures, *Computers & Structures*, 46(5), pp.905~916.

Roca, P., Mari, A.R. (1993b) Nonlinear Geometric and Material Analysis of Prestressed Concrete General Shell Structures, *Computers & Structures*, 46(5), pp.917~929.

Semblat, J.F., Aouameur, A., Ulm, F.J. (2004) Non Linear Seismic Response of a Low Reinforced Concrete Structure : Modeling by Multilayered Finite Shell Elements, *Structural Engineering and Mechanics*, 18(2), pp.211~229.

Smadi, M.M., Belakhdar, K.A. (2007) Nonlinear Finite Element Analysis of High Strength Concrete Slabs, *Computers & Concrete*, 4(3).

Talyor, R.L. (2000) *FEAP-A Finite Element Analysis Program, Version 7.2 Users Manual, Volume 1 and Volume 2.*

Wu, X.H., Otani, S., Shiohara, H. (2001) Tendon Model for Nonlinear Analysis of Prestressed Concrete Structures, *Journal of Structural Engineering*, ASCE, 127(4), pp.398~405.

Yamamoto, T., Vecchio, F.J. (2001) Analysis of Reinforced Concrete Shells for Transverse Shear and Torsion, *ACI Structural Journal*, 98(2), pp.191~200.

● 논문접수일 2010년 10월 16일
● 논문심사일 2010년 11월 12일
● 게재확정일 2010년 12월 6일